Analysis Of Pathological Lesions For Varicose Ulcer Classification Using Svm Classifier

R.R.Bhavani, Research Scholar, Manonmanaim Sundaranar Univeristy, Abishekapatti, Tirunelveli, TamilNadu, India, rrbme_2008@yahoo.co.in

Dr.G.Wiselin Jiji, Professor, Department of Computer Science and Engineering, Dr.Sivanthi Aditanar College of Engineering, Tiruchendur, Tamilnadu, India.

jijivevin@yahoo.co.in

Abstract - Any wound that penetrates deep into the tissues cause deviations in the distribution of cells, leading to changes in biological structures they form. Accurate identification of the affected tissue and analysing the characterization of these structures are essential for accurate diagnosis and classification of any ulcer. In this paper, we present a new approach for the classification of histopathological wound images of varicose ulcer stained with hematoxylin and eosin. The tissue image is decomposed into grid of non-overlapping images in order to perform classification in an efficient manner. Unlike other wound images pathology images are not easy to analyze for further processing. Hence features are extracted using some important matrices such as color edge graph and Delaunay Triangulation. Based on Color edge graph two important feature parameters namely Average Degree and Average Clustering coefficient and for Delaunay Triangulation three other parameters namely average, min-max ratio and standard deviation are used here. Classification is done in a much efficient manner by means of One vs All SVM classification. The experiments conducted on microscopic images of varicose wound tissues reveals that the structural features used here achieves higher classification accuracy than the previous approaches. Experiments conducted on 1546 photomicrographs of varicose ulcer tissues that are taken from 110 different patients demonstrate that the color graph approach leads to 98.63 % training accuracy and 97.77 % test accuracy.

Keywords – Varicose ulcer, Color Edge Graph, Delaunay triangulation, SVM classification

I. INTRODUCTION

A skin ulcer is an ailment that occurs when the skin tears down to reveal the underlying flesh. The most common type of skin ulcer is the Venous leg ulcer. Venous ulceration (stasis ulcer) is the most severe and debilitating outcome of chronic venous insufficiency in the lower limbs and accounts for 80 percent of lower extremity ulcerations [1]. Various other causes for lower extremity ulcerations could be arterial insufficiency, prolonged pressure, diabetic neuropathy and systemic illness such as rheumatoid arthritis, vasculitis, osteomyelitis, and skin malignancy [2]. Among various leg ulcers varicose ulcer accounts for over 90% of all cases. Venous ulcers are more commonly found in women and older persons and the threatening factors primarily include older age, obesity, previous leg injuries, deep venous thrombosis and phlebitis [3-7]. The incidence rate is 0.76% in men and 1.42% in women. Venous leg ulcers become more common as a person gets older and 20 in 1,000 people become affected by the time they are in their 80s. This disorder is widespread in every corner of rural, urban, developed, and underdeveloped parts of the world. About 1% of the population will be affected with a poorly healing lower extremity wound during their lifetime [8]. They are often recurrent and may sometimes persist from weeks to years, giving rise to the complications in form of cellulitis, osteomyelitis and at times malignant change [3, 9-11]. In spite of low overall prevalence, the refractory nature of these ulcers causes an increased risk of morbidity, mortality and a significant impact on quality of life [12, 13]. Venous hypertension, for a long period caused by venous insufficiency leads to venous ulceration. Lack of competent superficial veins and/or of perforators (because of direct injury, congenital abnormality or superficial inflammation) are the main reasons for 40% - 50% of venous leg ulcers. Deep venous system in these patients, function as normal [14]. For the treatment of leg ulcers the underlying pathology as well as the symptoms associated with the ulcer are essential. Digital images are sufficient for recognizing the case severity by experienced personnel. This indicates that digital pathological images of varicose ulcers can be used for any computer assisted techniques

 DOI : 10.18231/2454-9150.2018.1146

pointed out by works such as [15]. In [16], Erdem and Cigdem have addressed the classification model for digital pathology using structural and statistical pattern recognition. A broad literature survey has exposed the need for effective system of wound tissue classification, which might assist clinicians to treat the patients at an early stage for a faster healing rate. Delaunay triangulations have been used to build structural representations of various tissues for automated cancer diagnosis and grading. In [17], an automated framework that make use of Delaunay triangulations for grading of cervical intraepithelial neoplasia is proposed. In [18] Delaunay features were used for quantification of cervical tissues. In [19] an automated diagnosis and grading method for breast cancer that also employs Delaunay triangulations is proposed. Previous works on tissue classification [20] have been carried out using SVM classifier with an accuracy rate of 87%. Misclassification is a common problem in any classification algorithm. Jafari and Zadeh have proposed multiwavelet grading methodology for pathological images [21]. Various works have been carried out using histopathological images for the identification of many chronic diseases. [22-25]

Our research work on varicose ulcer classification is mainly done by using Delaunay triangulation method [26] earlier done on cancer tissues. Support Vector Machine (SVM) classifier is used in our work as it has high classifying accuracy and good capabilities of fault-tolerance and generalization.

II. VARICOSE ULCER AND HISTOPATHOLOGICAL APPROACHES

2.1 Stages of Varicose Veins

Classification of venous disease is important for standardization of venous disease reporting and characterization as well as for assessment of treatment effectiveness. For early detection and the correct treatment selection, knowing the stage of varicose ulcer is an important factor which decreases the recurrence rate to a great extent. In order to standardize the reporting and treatment of the diverse manifestations of chronic venous disorders, a comprehensive classification system (CEAP) is followed widely to allow uniform diagnosis and comparison of patient populations. The Clinical, Etiology, Anatomy, and Pathophysiology classification system (CEAP) is recommended for all patients with VLU for disease characterization. Figure 1 shows the pictorial representation of the varicose ulcer stages.

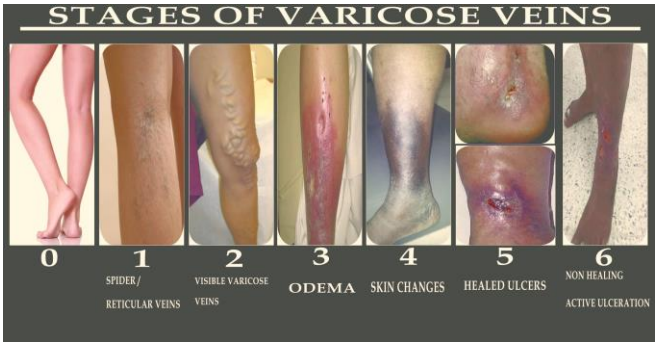

Figure 1 stages of Varicose Veins

In the proposed work class C6 is taken for study in which we have classified the Active Venous ulcer as Mild and severe comparing with the normal tissue. Accurate evaluation of varicose ulcers comprises of key factors like diagnosis, pathological evaluation and the symptoms and severity of each particular case. The main objective of focusing our work towards class C6 is this is the stage where patients face severe ill effects of the ulcer which may even end in the amputation of the leg. The earlier stages can be treated and also can be prevented from stepping into C6. But once the patients fall into this C6 stage they have to come under the complete observation of the clinicians. For the early diagnosis and timely treatment the clinicians are in need to identify whether the ulcer is in its mild or severe stage. To sort out this issue we have developed a computer assisted tool that will help the clinicians to identify the correct stage of the ulcer. Once the pathology image of the ulcer is given our system will classify it as mild or severe.

2.2 Earlier Works on Histopathological Images

Researchers are presently showing keen interest in developing methodologies for computerised classification of stromal and epithelial regions within H&E tissue images. Linder et al. in his work used local binary pattern (LBP) and contrast measure based texture features for discriminating epithelium and stroma from immunohistochemistry (IHC) stained tumor tissue microarrays (TMAs) of colorectal cancer [27]. Hiary et al. for his work on segmentation of stromal tissue of breast cancer used color based texture features extracted from square image blocks [28]. Eramian et al. proposed a binary graph cuts approach for segmenting EP and ST regions from odontogenic cysts images. In this method color histogram of these two regions were used for determining the graph weights [29]. Lahrmann et al. proposed a technique for discriminating tumor and stromal areas on immunofluorescence histological images. In this paper they have used a cell graph feature describing the topological distribution of the tissue cell nucle. [30], Super-pixel based algorithms play a major role in precise segmentation of any DICOM image. In a work by Beck et al. a super pixel based algorithm was used to over-segment breast tissue Hematoxylin and Eosin (H&E)

 DOI : 10.18231/2454-9150.2018.1146

images into small compartments. Subsequently the cell nuclei and cytoplasm within each smaller subcompartment were further classified into epithelial and stromal regions by a Support Vector Machine (SVM) classifier [31]. Also Ali et al. worked on a super pixel based SVM to separate EP from ST areas in tissue region so for opharyngeal squamous cell carcinoma in [32]. There are several more works on histopathological images by researchers. All these earlier works are based on widely used features such as color and texture. These feature descriptors usually simulate the visual perception of human pathologist in interpreting the tissue samples. The proposed methodology in this work has adopted Color Edge Graph and Delanuay triangulation for identifying the nodes and also extracted structural features based on the above two techniques. Furthermore the classifier used is SVM which is a powerful supervised classifier and accurate learning technique.

Various works have been putforth using computational methods that quantify the organizational properties of tissues. Researchers suggest mainly four different approaches for tissue quantification. Based on their principle of tissue quantification the approaches are classified as morphological, intensity-based, textural, and structural approaches. The morphological approach quantifies a tissue with the size and shape properties such as area, perimeter, roundness, and symmetry [33] of its cellular components. The intensity based approach quantifies a tissue with the gray level or color intensities of its pixels and this quantification process is done by calculating the histogram of the tissue image by putting its pixels into bins and defining features such as average, standard deviation, and entropy on the histogram [34]. In the textural approach, the texture of the entire tissue is characterized with a set of features such as those calculated from co-occurrence matrices [30]-[32],[3]5-[37], run-length matrices [36] and multiwavelet coefficients [21],[37]. Noise is the main issue in the textural approach. As far as a histopathological image is considered, there could be a large amount of noise arising from the staining and sectioning related problems [38]. The structural approach provides a higher level representation of a tissue using the spatial relationships and neighborhood properties of their cellular components. To this end, a graph is constructed on the cellular components and a set of local and global graph features is extracted. In literature, there are different methods of generating graphs. The most common method is to use Delaunay triangulations (and their corresponding Voronoi diagrams) where nuclear components of the tissue are considered as graph nodes [17]-[19], [35,38,40,41] Minimum spanning trees obtained from these graph based representations are also used for representation.

The major task of the proposed work is to classify the stages of ulcer. For this, the proposed methodology first describes the normal stage in terms of query graphs and defines the variations in the tissue components by identifying the regions whose subgraphs are most similar to the queried graphs. Subsequently it calculates the distance between the most similar subgraphs and the query graphs. The calculated distance and the structural features of the regions with morphological variations are used to classify the tissue image. The Delaunay triangulation method applied here only considers nuclear tissue components in structural representation. Delaunay triangulations are constructed on the centroids of the cell nuclei in which they use minimum spanning trees that are constructed by connecting the centroids of cell nuclei based on their Euclidean distance [17]-[19], [35,38],[40]-[42].

This paper is organized as follows. Section III describes the methodology of the proposed method. The experimental setup, performance analysis and the comparative study are dealt in Section IV. Finally, some conclusions and possible extensions of the proposed approach are discussed in the last section.

III. METHODOLOGY

The proposed approach for Varicose ulcer tissue image classification is implemented by constructing an attributed graph on its tissue components and describes the structure of a normal gland by means of a set of smaller query graphs. The subgraphs constructed is examined for variations in their structure over the entire tissue component and their correspondence with the normal gland. Structural features are extracted from these subgraphs to quantify tissue deformations, and hence, to classify the tissue. This approach includes three steps: node identification, graph generation (Delaunay Triangulation) for normal tissue images and with variations and feature extraction.

3.1 Histopathology Image Data Set

Varicose ulcer is nowadays very common among Indians which is not given adequate and timely attention and care. It has very adverse effects on the quality of life of a common man. The dataset used in this work is taken from the patients in and around the south zone of Tamilnadu, collected from Tirunelveli Medical College Hospital, Tirunelveli, Tamilnadu, India. . The tissue images that are used in the experiments are taken using a high resolution Digital Microscope. The image resolution affects the computational time required for processing a single image. Thus, the image resolution is selected as 480×640, which gives both accurate classification results and relatively lower computational times.

The database is composed of 1546 images clearly analysed and interpreted manually by experts into three categories. Once the infected tissue region is biopsied and evaluated

 DOI : 10.18231/2454-9150.2018.1146

under microscope pathologists confirm the presence of varicose ulcer and grade it as mild or severe.

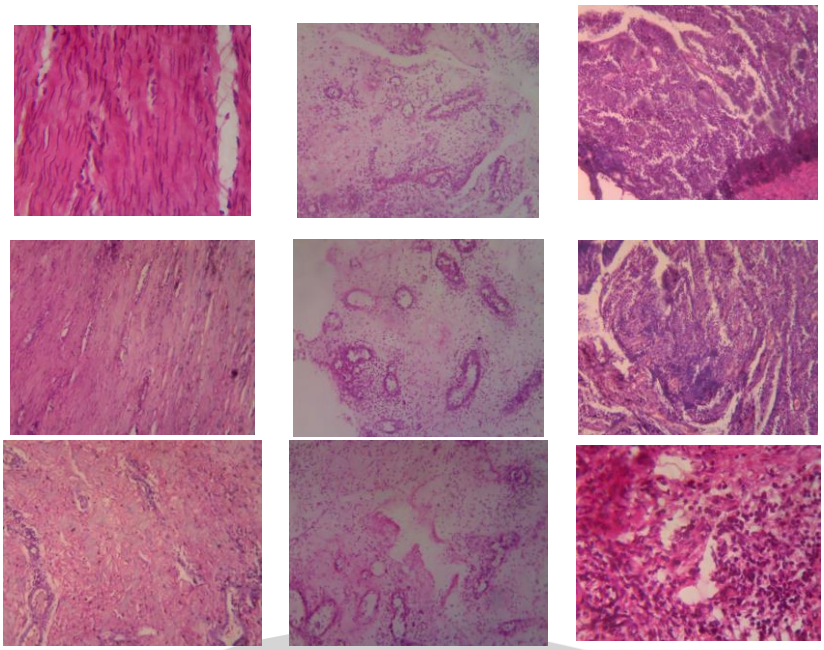

(a) Normal (b) Mild (c) Severe

Figure 2. Histopathological images of varicose ulcer tissues stained with the routinely used hematoxylin-and-eosin technique. (a) normal, (b) mild and (c) severe stages of varicose ulcer

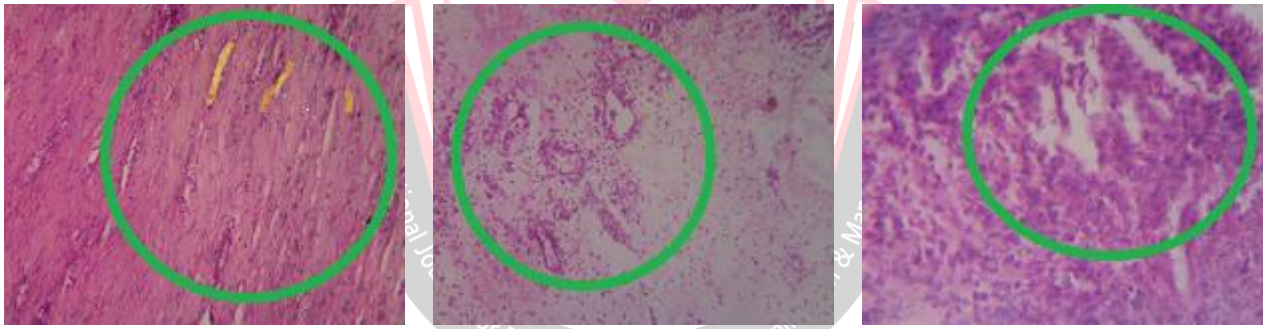

(a) (b) (c)

Figure 3. Histological tissue component variation between (i) normal, (ii) mild and (iii) severe stages of varicose ulcer

Figure 3 above shows the changes in the morphology and composition of the tissue components in the histopathological images of normal, mild and severe stages of varicose ulcer. From the figure, it is clearly understood that the even distribution of cellular components in the normal tissue (a) gets irregular slightly in the mild stage (b) and even more in the severe stage(c). In the normal tissue the cells are in close proximity surrounded by a fine layer of amorphous fibrous tissue and separated by regularly arranged collagen fibre bundles whereas in the varicose ulcer tissue the cells appear to be separated from each other by a marked increase in the fibrous tissue separated by grossly irregular collagen fibres. The degree of variations in these structures is the indicator of the ulcer stage. The precise identification of the variations and their correct quantification are very essential for the classification of the stages of ulcer.

3.2 Proposed Methodology

The proposed method develops a computer assisted tool to diagnosis the correct stage of the varicose ulcer in class C6. Figure 4 shows the block diagram of the proposed work.

 DOI : 10.18231/2454-9150.2018.1146

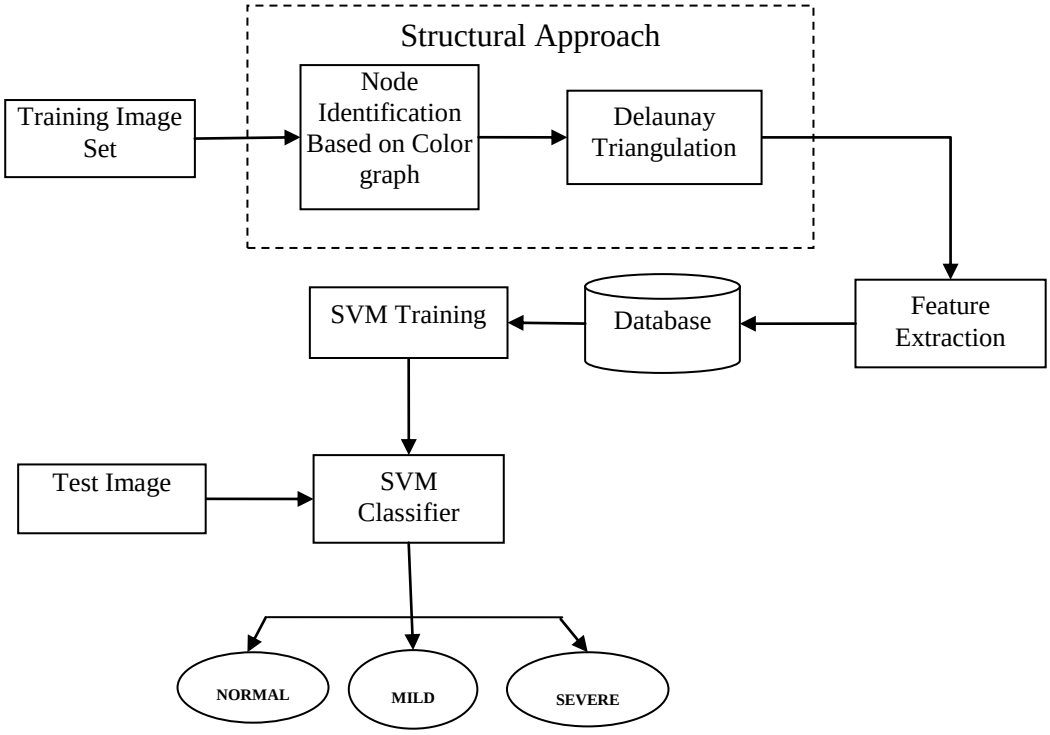

Fig 4: Block Diagram of the Proposed Work

This paper presents a structural method using Delaunay Triangulation to mathematically represent and quantify a tissue for the purpose of classifying the stages of Varicose Ulcer. This structural method was previously used for cancer diagnosis and grading. The proposed approach models a tissue image by constructing an attributed graph on its tissue components and describes what a normal gland is by defining a set of smaller query graphs. Unlike the previous structural methods, which quantify a tissue considering the spatial distributions of its cell nuclei, our proposed method relies on the use of distributions of multiple tissue components for the representation. To this end, it constructs a graph on multiple tissue components and colors its edges depending on the component types of their endpoints. Subsequently, it extracts a new set of structural features and uses these features in the classification of tissues.

The proposed methodology includes the following steps: Color Graph (Node Identification), Delaunay Triangulation, Feature extraction and Classification using SVM classifier.

3.2.1 Color Graph

The main objective of using color graphs in this work is to identify the extent of changes in the histopathological images of normal, mild and severe stages of varicose ulcer. The proposed approach considers the morphological changes in the tissue components and constructs a color graph for a tissue image by considering these changes and assigns edges between the positions where the components vary in their morphology by making use of Delaunay triangulation. Node identification and Edge assignment are explained in the following section.

3.2.1.1 Node Identification

Normally color graphs are used for assignment of labels (i.e) colors to elements of a graph subject to certain constraints. Here in the proposed work the color graph approach takes all components of a tissue with morphological changes into account to effectively quantize its histopathological image. In this the nuclear, stromal, and luminal components of a tissue are mapped to graph nodes. To perform this mapping, we have segmented the histopathological images into its cytological components. The segmentation is ideally performed by identifying the exact boundaries of each component. The common issues encountered in histopathological images are staining and sectioning related problems which includes wrinkled or compressed sections, cutting thick and thin sections, obtaining a section from tissues which are often brittle after processing and also the existence of touching and overlapping components. Other issues like non prevalence of thick separation lines between a component and its surroundings, non-homogeneity in the interior of a component, and presence of the residuals of stain particles in a tissue also exist. This complex nature of a histopathological image scene leads to a difficult segmentation problem even for the human eye. To overcome these issues the proposed methodology takes into consideration the tissue components where the morphological changes exist. The centroids of these tissue components are considered as the node locations in constructing a color graph. The nodes interconnect the

 DOI : 10.18231/2454-9150.2018.1146

locations where the tissue components vary in their structure. For each type of tissue normal, mild and severe the node points locate their structural differences. Thus the color graph generated clearly distinguishes the three types of tissues based on their components where they differ in their morphology.

The distinction shown in the node points in this step is very important for applying Delaunay Triangulation method on these images. Only the variation in node points distinguish the three types of tissue images.

3.3 Delaunay Triangulation

After identifying the nodes edge assignment is the next step to be performed. Our proposed methodology constructs Delaunay triangulation on the identified nodes. Delaunay Triangulation is used to build structural features on the tissue components. So it only considers nuclear tissue components in its structural representation. Thus, it ignores the existence of different components in the tissue. We employ this method to examine the effects on morphological variations in the tissue components in a structural representation. In our work the Delaunay triangulation is defined as the set of triangles where each triangle is generated from the nodes identified based on the variations in their tissue components. This variation conforms to the condition that the three types of tissue images (i.e) normal, mild and severe differ in their structural representation. Earlier nodes have been identified in this respect and therefore the Delaunay Triangulation also constructs graph in the same manner. The condition of Delaunay guaranties that each triangle of the triangulation clearly separates the morphologically different regions in the tissue images for all three cases.

We employ this method to examine the effects of considering luminal and stromal tissue components in a structural representation.

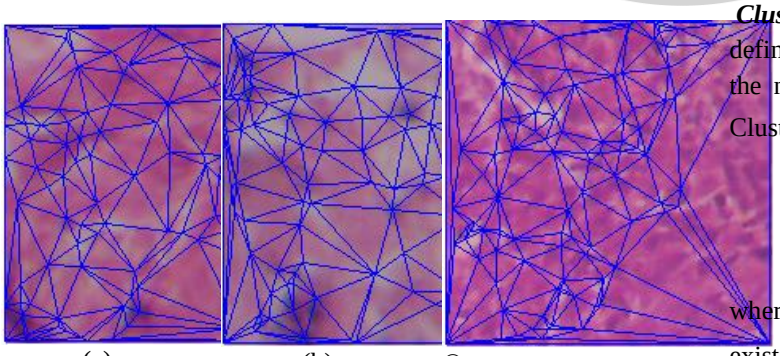

(a) (b) ©

Figure 5. Delaunay Triangulations constructed on Histopathological Images of (a) Normal (b) Mild and (c) Severe stages of Varicose Ulcer

Figure 5 (a, b, c) shows the Delaunay triangulations that are constructed on the normal, mild and severe stages of varicose ulcer tissue images taken from the dataset.

The graph generated on the tissue images clearly distincts the stromal and luminal parts. This distinction is mainly used to classify the tissue images. The Delaunay triangulation applied on the histopathological image of varicose ulcer makes the classification more efficient.

3.4 Feature extraction

In pattern recognition and in image processing, feature extraction is a special form of dimensionality reduction. When the input data to an algorithm is too large to be processed and it is suspected to be notoriously redundant then the input data will be transformed into a reduced representation set of features. Transforming the input data into the set of features is called feature extraction. If the features extracted are carefully chosen it is expected that the features set will extract the relevant information from the input data in order to perform the desired task using this reduced representation instead of the full size input. In our work the features extracted are (i) Average Degree, (ii) Average Clustering Coefficient, (color edge graph) [43] (iii) Average, (iv) Min Max Ratio and (v) Standard Deviation (Delaunay Triangulation) [44].

3.4.1 Features for Color Edge Graph:

(i) Average Degree:

In graph theory, the degree of a node is defined as the number of its adjacent neighbors. The average degree of a graph is the mean of the degrees computed for every node in the graph.

(ii) Average Clustering Coefficient

Average clustering coefficient also provides information about the connectivity of a graph. It indicates the density of connections in the neighborhood of a node. For an individual color graph, clustering coefficients are computed using the following definitions:

Clustering coefficient: Clustering coefficient of a node is defined as the ratio of the number of existing edges over the number of all possible edges between its neighbors. Clustering coefficient C_i of node *i* is computed as follows:

$$C_i = \frac{2d_i \cdot E_i}{d_i(d_i - 1)} \qquad (1)$$

where d_i is the degree of *i* and E_i is the number of existing edges between its neighbors.

Averaging the clustering coefficients over all nodes, four global features are obtained to quantify a color graph.

3.4.2 Features for Delaunay Triangulation:

(iii) Average:

Average is defined as the mean between the edges of triangles and its distance according to Delaunay

 DOI : 10.18231/2454-9150.2018.1146

Triangulation. At first all the sides of the triangle are being computed and then min-max ratio is being formed.

(iv) Min-Max Ratio:

Min-Max ratio is defined as the minimum and maximum of edges in a triangle based on the Delaunay Triangulation. At first all the sides of the triangle are being computed and then min-max ratio is being formed.

(v) *Standard Deviation*:

Standard deviation is a measure that is used to quantify the amount of variation or dispersion of a set of data values. A low standard deviation indicates that the data points tend to be close to the mean (also called the expected value) of the set, while a high standard deviation indicates that the data points are spread out over a wider range of values based on the edges of the triangle.

3.5 Classification using SVM Classifier

SVM is a widely adopted supervised classifier for its high precision. It founds its root from the statistical theory developed by Vapnick in 1982 [45]. It has records of effective classification results in many application domains, e.g. medical diagnosis [46, 47]. The major task of a support vector machine is to find an ideal separating hyper-plane between members and non-members of a specified class in a high dimension feature space [48]. SVM performs classification in one of the following two ways ONE vs ALL or ONE vs ONE. The ONE vs ALL strategy distinguishes the samples of one class from the samples of remaining classes and ONE vs ONE is done in pairs where one SVM is constructed for each pair of classes. For n classes, $n(n-1)/2$ SVMs are trained to distinguish the samples of one class from the samples of another class. Both strategies are for unknown patterns and the difference lies therein whether the classification of an unknown pattern is done according to the maximum output among all SVMs (ONE vs ALL) or classification of an unknown pattern is done according to the maximum voting , where each SVM votes for one class (ONE vs ONE). In our proposed work we have adopted ONE vs ALL so that each stage of the ulcer is classified into a separate class namely Normal, Mild and Severe.

The features extracted from color edge graph and Delaunay triangulation are the inputs to the SVM algorithm. In this work, we have focused on the classification of normal and varicose ulcer tissues. Then the classification further proceeds to divide the varicose ulcer tissues into mild and severe. The dataset consists of histopathological images of normal, mild and severe stages of Varicose ulcer. Based on random sampling method the dataset is divided into training and test sets. A total of 45 cases were involved in training the system comprising of 826 images (240 - Normal stage, 250 - Mild stage and 336-Severe stage). The test set consists of 65 cases comprising of 720 images (180- Normal Stage, 220- Mild Stage and 320- Severe Stage). The experiment is conducted on 720 samples of testing set out of which 3 classes are extracted. There are many common kernel functions, such as:

- Linear: $X_i - X_j$
- Polynomial of degree $d : (X_i \cdot X_j + 1)^d$
- Radial basis function (RBF):

$$\exp\left[\frac{-\|X_i - X_j\|^2}{2\sigma^2}\right]$$

The radial basis function is found to be the best due to the fact the vectors are nonlinearly mapped to a very high dimension feature space. The optimal values of constants γ and C are determined, where γ is the width of the kernel function and C is the error/trade-off parameter that adjusts the importance of the separation error in the creation of the separation surface. We perform the classification for the varicose ulcer dataset with (γ, C) varying along a grid. SVM-based classification takes N training samples, trains the classifier on N-1 samples, then uses the remaining one sample to test. This procedure is repeated until all N samples have been used as the test sample. The performance of the classification for a given value (γ, C) is evaluated by computing the accuracy across all subjects.

The features extracted from Color graphs and Delaunay triangulation are used by the SVM classifier for efficient classification of varicose ulcer tissue images.

IV. EXPERIMENTAL RESULTS

This section describes the experimental methodology and provides the results of the proposed approach for a three class classification problem of varicose ulcer. The experiments were conducted on the native collected varicose ulcer tissue images. The images were studied under the guidance of clinicians to identify the correct stage of wound. Using color graph and Delaunay triangulation the structural features are extracted and the different stages are classified using SVM classifier. The proposed system is implemented using the tool MATLAB 2013. The training and testing was carried out in the Windows 8.1 PC configured by Intel Core I3 CPU 2.3 GHz, 2 GB RAM and 250GB storage.

4.1 *Classification Results:*

This section gives the results for the classification of these types of tissues using support vector machines (SVM). The confusion matrices are given for the classification of training and test data with the use of 5 features computed from color graphs and Delaunay Triangulation.

 DOI : 10.18231/2454-9150.2018.1146

		Classified Tissue		
		Normal	Mild	Severe
Training Set	Normal	233	4	3
	Mild	5	241	4
	Severe	4	4	328

(a)

		Classified Tissue		
		Normal	Mild	Severe
Test Set	Normal	174	3	3
	Mild	4	210	6
	Severe	3	5	312

(b)

Table 1: Confusion matrices obtained with the structural features for color graph and Delaunay Triangulation for (a) training set and (b) test set

In Table I, we provide the confusion matrices obtained on the training and test sets. From the confusion matrices it is clear that the proposed approach yields good results for both the training and test sets. The classification result for all classes in the training set are also precise. It is also clear from the matrices that although the proposed approach leads to higher accuracies for the classification of the normal and severe stages of varicose ulcer, it gives relatively lower accuracies for the mild stage of varicose ulcer. To rule out this issue we check the misclassifications for all the three classes. Figure 7 shows the outputs of the misclassification results for normal, mild and severe stages of varicose ulcer.

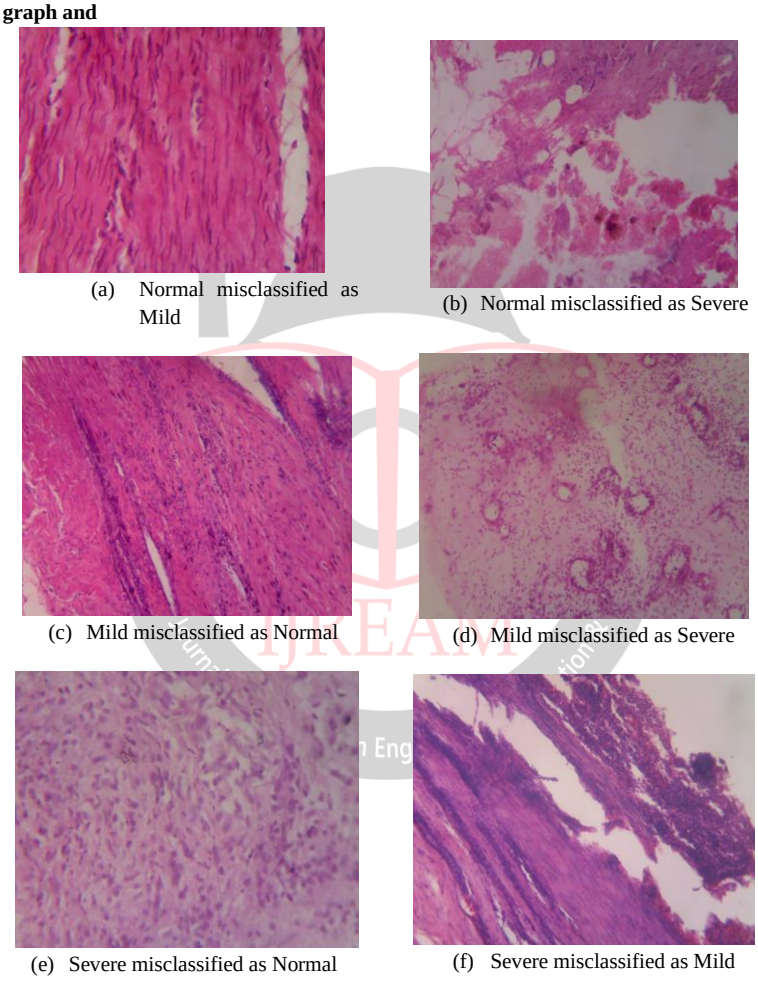

(a) Normal misclassified as Mild
(b) Normal misclassified as Severe
(c) Mild misclassified as Normal
(d) Mild misclassified as Severe
(e) Severe misclassified as Normal
(f) Severe misclassified as Mild

Figure 6. Varicose ulcer (a)-(b) Normal, (c)-(d) Mild and (e)-(f) Severe tissue images misclassified by the proposed approach

The observation leads to the fact that almost all of the normal tissues that are misclassified as mild (6a) comprise staining related problems commonly found in any histopathological image. In addition to this, almost all of the normal tissues that are misclassified as severe (6b) consist of sparsely located glands. Examples of misclassified mild tissues are given in Figure 6c and 6d. This misclassification is not much erroneous and it lies at the boundary between mild and severe stages. Figure 6e and Figure 6f show the examples of misclassified severe stage samples which does not show any common characteristics.

4.2 **Performance assessment metrics**

The True Positive Value (i.e) the percentage of correctly identified ulcer stage is used to find the Sensitivity of the proposed method.

 DOI : 10.18231/2454-9150.2018.1146

$$Sensitivity = \frac{NoOfCasesIdentifiedExactlyAtItsCorrectStage}{NoOfcasesIdentifiedCorrectlyAtItsCorrectStage + NoOfCasesNotIdentifiedInCorrectlyAtItsCorrectStage} \quad (2)$$

The True Negative predictions are used to calculate the Specificity value. False positive rate is the percentage of ulcer stages correctly rejected by our system as not reported clinically. In rare cases, the specificity would be useful to detect the correct stage misinterpreted clinically.

$$Specificity = \frac{NoOfCasesRejectedExactlyAtItsInCorrectStage}{NoOfCasesRejectedExactlyAtItsInCorrectStage + NoOfCasesIdentifiedInCorrectlyAtItsCorrectStage} \quad (3)$$

Accuracy is the measure which gives the predictive ability of the proposed system in terms of True Positive, True Negative, False Positive and False Negative values.

$$Accuracy = \frac{TruePositive + TrueNegative}{TruePositive + TrueNegative + FalsePositive + FalseNegative} \quad (4)$$

These three different performance measures shown in equation (2) – (4) are used to quantify the proposed system and other comparative works.

Table 2 gives the performance measures of the proposed work for both the training and test set.

Class/ Performance Measures	Training Set					Test Set				
	Sensitivity	Specificity	Precision	Accuracy	F score	Sensitivity	Specificity	Precision	Accuracy	F score
1	0.9628	0.9880	0.9708	0.9806	0.9668	0.9613	0.9888	0.9666	0.9819	0.9639
2	0.9678	0.9844	0.9640	0.9794	0.9659	0.9633	0.9800	0.9545	0.9750	0.9589
3	0.9791	0.9837	0.9761	0.9818	0.9776	0.9719	0.9799	0.9750	0.9763	0.9734
Average	**0.9699**	**0.9853**	**0.9703**	**0.9806**	**0.9701**	**0.9655**	**0.9829**	**0.9654**	**0.9777**	**0.9654**

Table 2: Performance measures of the proposed work for both the training and test set

The above table shows that on an average the proposed work yields good classification result for both the training and test set. Figure 8 shows the graphical representation of the performance analysis of the proposed work.

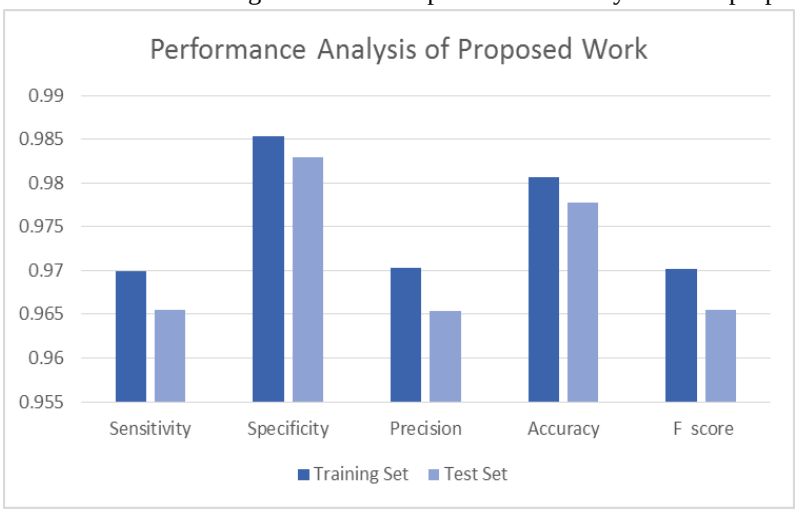

Figure 7. Performance Analysis of the proposed work

 DOI : 10.18231/2454-9150.2018.1146

For comparison the state-of-art methods proposed by Dogan Altunbay et al (2010) are applied on our native dataset and the accuracy analysis results are shown in Table 3.

Class	Proposed Work					Dogan Altunbay et al(2010)				
	Sensitivity	Specificity	Precision	Accuracy	F score	Sensitivity	Specificity	Precision	Accuracy	F1 Score
1	0.9613	0.9888	0.9666	0.9819	0.9640	0.9334	0.9589	0.9423	0.9635	0.9597
2	0.9633	0.9800	0.9545	0.9750	0.9589	0.9544	0.9775	0.9558	0.9567	0.9426
3	0.9719	0.9799	0.9750	0.9763	0.9735	0.9873	0.9714	0.9314	0.9715	0.9338
Average	**0.9655**	**0.9829**	**0.9654**	**0.9777**	**0.9655**	**0.9584**	**0.9693**	**0.9432**	**0.9639**	**0.9454**

Table 3: Statistical performance measures of proposed work along with the comparative work.

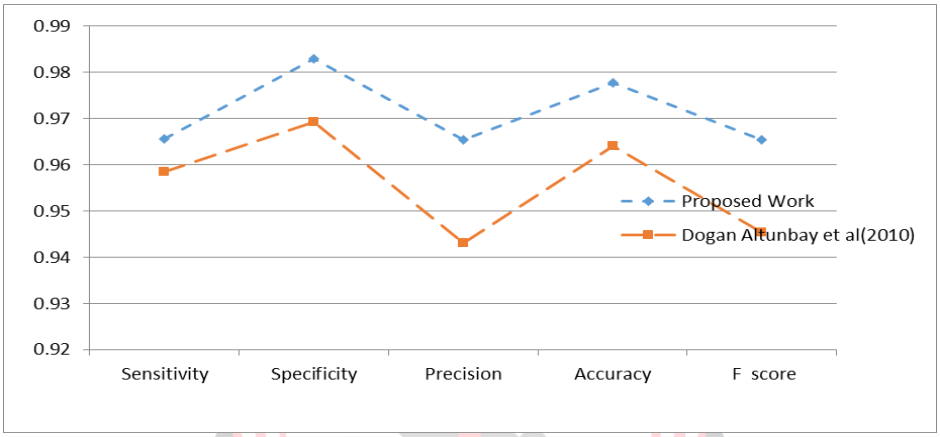

Figure 8: Comparative Accuracy analysis of the proposed work with the work proposed by Dogan Altunbay et al. (2010)

Figure 9 shows the comparative accuracy analysis of the proposed method with earlier method proposed by Dogan Altunbay et al. (2010). While experimenting the results, the proposed method attains 96.55 % sensitivity, 98.29 % specificity, 96.54 % precision, 97.7 % accuracy and 96.55 % F score.

V. CONCLUSION

Computer aided image analysis for varicose ulcer tissue classification is much needed nowadays for early diagnosis and treatment. This analysis makes use of computational methods that employ various image processing techniques. The methods presently in use ignore the existence of other components in a histopathological image such as luminal and stromal regions. These regions play crucial role in the tissue structure. In this thesis, we introduce a new structural method for automated varicose ulcer grading. This method involves color graph and Delaunay Triangualtion approaches to extract the structural features from the tissue images. These extracted features are used by support vector machines for classification.

We conducted the experiments on 1546 photomicrographs of varicose ulcer tissues that are taken from 110 different patients. These experiments demonstrate that the structural features lead to 98.63 % training accuracy and 97.77 % test accuracy for the varicose ulcer tissue classification. The proposed method shows that the effectiveness of the approach is improved by considering different tissue components in a structural representation. As Delaunay triangulation is known to be one of the effective representations in quantifying the spatial distribution of graph nodes we propose it for graph generation. The experiments conducted on the varicose ulcer tissue images demonstrate that the colored features lead to improved test accuracy for the automated varicose ulcer classification. As our approach is fully based on the structural features it gives better results when compared to its counterparts.

REFERENCES

[1] O'Meara S, Al-Kurdi D, Ologun Y, Ovington LG., "Antibiotics and Antiseptics for Venous Leg Ulcers," Cochrane Database Syst Rev. 2010 Jan 20;(1):CD003557

[2] T. de Araujo, I. Valencia, D. G. Federman and R. S. Kirsner, "Managing the Patient with Venous Ulcers," Annals of Internal Medicine, Vol. 138, No. 4, 2003, pp. 326-334.

[3] L. P. Abbade and S. Lastória, "Venous Ulcer: Epidemiology, Physiopathology, Diagnosis and Treatment," International Journal of Dermatology,

 DOI : 10.18231/2454-9150.2018.1146

Vol. 44, No. 6, 2005, pp. 449-456. doi:10.1111/j.1365-4632.2004.02456.x

[4] M. J. Callam, D. R. Harper, J. J. Dale and C. V. Ruckley, "Chronic Ulcer of the Leg: Clinical History," British Medical Journal, Vol. 294, No. 6584, 1987, pp. 1389-1391.

[5] D. Bergqvist, C. Lindholm and O. Nelzén, "Chronic Leg Ulcers: The Impact of Venous Disease," Journal of Vascular Surgery, Vol. 29, No. 4, 1999, pp. 752-755.

[6] Aziz Z1, Cullum N, Flemming K, "Electromagnetic Therapy for Treating Venous Leg Ulcers," Cochrane Database Syst Rev. 2013 Feb 28;(2):CD002933.

[7] Nelson EA1, Bell-Syer SE., "Compression for Preventing Recurrence of Venous Ulcers," Cochrane Database Syst Rev. 2014 Sep 9;(9):CD002303.

[8] Deborah A Simon, Francis P Dix and Charles N McCollum, Management Of Chronic Venous Leg Ulcers: BMJ. 2004 Jun 5; 328(7452): 1358–1362.

[9] M. Briggs and E. A. Nelson, "Topical Agents or Dressings for Pain in Venous Leg Ulcers," Cochrane Database Syst Rev. 2010 Apr 14;(4):CD001177.

[10] O. Nelzén, D. Bergqvist and A. Lindhagen, "Long-Term Prognosis for Patients with Chronic Leg Ulcers: A Prospective Cohort Study," European Journal of Vascular & Endovascular Surgery, Vol. 13, No. 5, 1997, pp. 500-508.

[11] R. H. Samson and D. P. Showalter, "Stockings and the Prevention of Recurrent Venous Ulcers," Dermatologic Surgery, Vol. 22, No. 4, pp. 373-376.

[12] M. J. Callam, C. V. Ruckley, D. R. Harper and J. J. Dale, "Chronic Ulceration of the Leg: Extent of the Problem and Provision of Care," British Medical Journal, Vol. 290, No. 6485, 1985, pp. 1855-1856. doi:10.1136/bmj.290.6485.1855

[13] C. V. Ruckley, "Socioeconomic Impact of Chronic Venous Insufficiency and Leg Ulcers," Angiology, Vol. 48, No. 1, 1997, pp. 67-69. doi:10.1177/000331979704800111

[14] J. Grey, K. Harding and S. Enoch, "ABC of Wound Healing: Venous and Arterial Leg Ulcers," British Medical Journal, Vol. 332, 2006, p. 7537.

[15] J. Cuddigan, E. Ayello, And C. Sussman, Eds., "Pressure Ulcers In America: Prevalence, Incidence, And Implications For The Future", **Advances in Skin & Wound Care: The Journal for Prevention and Healing,** July/August 2001, Volume: 14 Number 4 , page 208 - 215

[16] Erdem Ozdemir and Cigdem Gunduz-Demir, A Hybrid Classification Model for Digital Pathology Using Structural and Statistical Pattern Recognition, IEEE Transactions on Medical Imaging, Vol. 32, No. 2, February 2013.

[17] S. J. Keenan, J. Diamond, G. W. McCluggage, H. Bharucha, D. Thompson, P. H. Bartels, and P. W. Hamilton. An automated machine vision system for the histological grading of cervical intraepithelial neoplasia (CIN). The Journal of Pathology, 192(3):351–362, 2000.

[18] M. Guillaud, D. Cox, K. Adler-Storthz, A. Malpica, G. Staerkel, J. Matisic,D. Van Niekerk, N. Poulin, M. Follen, and C. MacAulay. Exploratory analysis of quantitative histopathology of cervical intraepithelial neoplasia: Objectivity, reproducibility, malignancy-associated changes, and human papillomaavirus. Cytometry, 60A(1):81–9, 2004.

[19] S. Doyle, S. Agner, A. Madabhushi, M. Feldman, and J. Tomaszewski, "Automated grading of breast cancer histopathology using spectral clustering with textural and architectural image features," in Proc. Biomed Imag.: From Nano to Macro, 2008, pp. 496–499..

[20] Lei Wang, Peder C. Pedersen , Emmanuel Agu , Diane Strong , Bengisu Tulu, "Area determination of diabetic foot ulcer images using a cascaded two-stage SVM-based classification", IEEE Trans. Biomed. Eng., vol. 64, no. 9, pp. 2098-2109, Sep. 2017.

[21] K. Jafari-Khouzani and H. Soltanian-Zadeh, "Multiwavelet grading of pathological images of prostate," IEEE Trans. Biomed. Eng., vol. 50, no. 6, pp. 697–704, Jun. 2003

[22] B. Tosun and C. Gunduz-Demir, "Graph run-length matrices for histopathological image segmentation," IEEE Trans. Med. Imag., vol. 30, no. 3, pp. 721–732, Mar. 2011.

[23] Tabesh, M. Teverovskiy, H. Y. Pang, V. P. Kumar, D. Verbel, A. Kotsianti, and O. Saidi, "Multifeature prostate cancer diagnosis and Gleason grading of histological images," IEEE Trans.Med. Imag., vol. 26, no. 10, pp. 1366–1378, Oct. 2007.

[24] P.-W. Huang and C.-H. Lee, "Automatic classification for pathological prostate images based on fractal analysis," IEEE Trans. Med. Imag., vol. 28, no. 7, pp. 1037–1050, Jul. 2009.

[25] Wang W, Ozolek JA, Rohde GK. Detection and Classification of Thyroid Follicular Lesions Based on Nuclear Structure from Histopathology Images. Cytometry Part A : the journal of the International Society for Analytical Cytology. 2010;77(5):485-494. doi:10.1002/cyto.a.20853.

[26] D. Altunbay, C. Cigir, C. Sokmensuer, and C. Gunduz-Demir, "Color graphs for automated cancer

 DOI : 10.18231/2454-9150.2018.1146

diagnosis and grading," IEEE Trans. Biomed. Eng., vol. 57, no. 3, pp. 665–674, Mar. 2010.

[27] N.Linder, et al., Identification of tumor epithelium and stroma in tissue microarrays using texture analysis, Diagn .Pathol. 7(1)(2012)22,URL

[28] H.Hiary,etal.,Automated segmentation of stromal tissue in histology images using a voting Bayesian model, Signal Image Video Process. 7(6)(2013) 1229–1237,URL

[29] M. Eramian, et al., Segmentation of epithelium in H&E stained odontogenic cysts, J.Microsc.244(3)(2011)273–292.

[30] B. Lahrmann, N.Halama, H.-P.Sinn, P.Schirmacher, D.Jaeger, N.Grabe, Automatic tumor-stroma separation in fluorescence TMAs enables the quantitative high-throughput analysis of multiple cancer biomarkers, PLoSOne6 (December (12)) (2011) e28048.

[31] A.H. Beck, et al., Systematic analysis of breast cancer morphology uncovers stromal features associated with survival, Sci. Transl. Med. 3 (2011) 108ra113

[32] S.Ali, et al.,Spatially aware cell clusters graphs: predicting outcome in HPV associated oropharyngeal tumors, in: Medical Image Computing and Computer-AssistedIntervention,vol.8149,2013,pp.412–519

[33] W. N. Street, W. H. Wolberg, and O. L. Mangasarian, "Nuclear feature extraction for breast tumor diagnosis," IS&T/SPIE 1993 International Symposium on Electronic Imaging: Science and Technology, volume 1905, pages 861-870.

[34] M. Wiltgen, A. Gerger, and J. Smolle, "Tissue counter analysis of benign common nevi and malignant melanoma," Int. J. Med. Inf., vol. 69, pp. 17– 28, 2003.

[35] S. Beura, et al., Mammogram classification using two dimensional discrete wavelet transform and gray-level co-occurrence matrix for detection of breast cancer, Neurocomputing (2015),

[36] Esgiar, R. Naguib, B. Sharif, M. Bennett, and A. Murray, "Microscopic image analysis for quantitative measurement and feature identification of normal and cancerous colonic mucosa," IEEE Trans. Inf. Technol. B, vol. 2, no. 3, pp. 197–203, Sep. 1998.

[37] O. Sertel, J. Kong, H. Shimada, U. V. Catalyurek, J. H. Saltz, and M. N. Gurcan, "Computer-aided prognosis of neuroblastoma on wholeslide images: Classification of stromal development," Pattern Recognit., vol. 42, no. 6, pp. 1093–1103, 2009.

[38] Weyn, G. van de Wouver, M. Koprowski, A. van Daele, K. Dhaene, P. Scheunders, W. Jacob, and E. van Marck, "Value of morphometry, texture analysis, densitometry, and histometry in the differential diagnosis and prognosis of malignant mesothelia,"J. Pathol., vol. 189, pp. 581–589, 1999.

[39] J. Gil, H. Wu, and B. Y. Wang, "Image analysis and morphometry in the diagnosis of breast cancer," Microsc. Res. Tech., vol. 59, pp. 109–118, 2002.

[40] Weyn, G. van de Wouwer, S. Kumar-Singh, A. Van Daele, P. Scheunders, E. van Marck, and W. Jacob, "Computer-assisted differential diagnosis of malignant mesothelioma based on syntactic structure analysis," Cytometry, vol. 35, pp. 23–29, 1999.

[41] J. Sudbo, R. Marcelpoil, and A. Reith, "New algorithms based on the Voronoi diagram applied in a pilot study on normal mucosa and carcinomas,"Anal. Cell. Pathol., vol. 21, pp. 71–86, 2000.

[42] H.-K. Choi, T. Jarkrans, E. Bengtsson, J. Vasko, K. Wester, P.-U. Malmstrom, and C. Busch, "Image analysis based grading of bladder carcinoma. Comparison of object, texture and graph based methods and their reproducibility," Anal. Cell. Pathol., vol. 15, pp. 1–18, 1997

[43] E Ozdemir, C Sokmensuer, C Gunduz-Demir, "A resampling-based Markovian model for automated colon cancer diagnosis", IEEE transactions on biomedical engineering 59 (1), 281-289

[44] S. Doyle, S. Agner, A. Madabhushi, M. Feldman, and J. Tomaszewski, "Automated grading of breast cancer histopathology using spectral clustering with textural and architectural image features," in Proc. 5th IEEE Int. Symp. Biomed Imaging: From Nano to Macro, Paris, May. 14–17, 2008, pp. 496–499.

[45] Vapnik V.N., Estimation of Dependences Based on Empirical data, Secaucus, NJ, USA, Springer-Verlag New York, 1982.

[46] Guyon I., Weston J., Barnhill S., Vapnik V., Gene Selection for Cancer Classification using Support Vector Machines, Machine Learning, 2002, 46(1-3), p. 389-422.

[47] Zhang J., Liu Y., Cervical Cancer Detection Using SVM Based Feature Screening, Proc of the7th Medical Image Computing and Computer-Assisted Intervention, 2004, 2, p.873-880

[48] Kim D., Park J., Network-based intrusion detection with support vector machines, Lecture Notes in Computer Science, 2003, 2662, p. 747-756

 DOI : 10.18231/2454-9150.2018.1146